XENON RESISTOJET DESIGN AND DEVELOPMENT

Kent T. Chojnacki and Robert Reinicke
Space Products Division
Moog, Inc.
East Aurora, NY 14052-0018

Abstract

Moog, Inc. has designed and performed development testing on a resistojet intended for use with xenon propellant. Performance data were collected for both nitrogen and xenon propellants at power levels up to 70 W and mass flow rates between .0085 and .4224 g/s. The maximum achieved specific impulse for nitrogen was 115.2 s and the highest achieved specific impulse for xenon was 66.9 s at the highest power settings.

Introduction

The use of xenon-fueled electrostatic propulsion systems is expanding. While these propulsion systems are attractive for station keeping and orbit transfer applications, they are not appropriate for low ΔV missions such as attitude control. Traditional propulsion options exist to fulfill these low ΔV needs. Nitrogen cold gas thrusters and hydrazine mono-propellant thrusters (including resistojets and arcjets) are well characterized and have extensive flight experience. However, the use of either of these propulsion options requires the spacecraft to be equipped with two separate propellant management systems. Cold gas thrusters or resistojets which utilize xenon propellant would allow a one-propellant spacecraft with substantial mass savings by eliminating redundant tankage and propellant control hardware. This would be off-set by a substantial reduction in performance compared to the traditional propellant options. This needs to be the subject of spacecraft-level trade studies to determine the preferred solution.

Xenon resistojet performance is more attractive than xenon cold gas propulsion. Published results show that xenon cold gas specific impulse can be almost doubled by relatively modest power inputs (<10 W)[1]. However, the literature yields little other data on cold gas thruster or resistojet performance with xenon propellant. In order to aid spacecraft-level trade studies, extensive data are required on these propulsion options.

Moog, Inc. has designed and performed development testing on a resistojet intended for use with xenon propellant. The goals of the program were two-fold: 1) Design a resistojet that would meet a set of predetermined performance goals; and 2) Concentrate on design options which would yield a low-cost, highly producible design.

Xenon resistojets can be run in two modes: a continuous mode where the heater is held at full power and gas is continuously flowing; and a pulse mode of operation whereby the heater can be run in a pre-heat cycle and the valve portion of the resistojet pulsed to produce small impulse bits. The paper presented herein addresses Moog's development efforts with respect to continuous mode operation. No results are presented for any type of pulsing mode. The key continuous operation performance goals are summarized in Table 1.

Table 1: Continuous Operation Mode Performance Goals

Parameter	Moog Imposed Design Goal
MEOP	2.1 bar (30.5 psia)
Thrust	220 mN
Maximum Xe Flow Rate	0.4 g/s
Continuous Mode Specific Impulse (with Full Heater Power)	50 sec
Resistojet Power Consumption	80 W (max)
Internal Leakage	$<5 \times 10^{-5}$ scc/s GHe at 2 bar differential
Total Resistojet Mass	200 g (max)

The paper describes key aspects of Moog's resistojet design, provides analysis and

experimental results of the resistojet heat exchanger, and presents experimental thrust and specific impulse data for both nitrogen and xenon propellants.

Resistojet Design

The Moog model 50X914 resistojet is shown pictorially in Figure 1 and dimensionally in Figure 2.

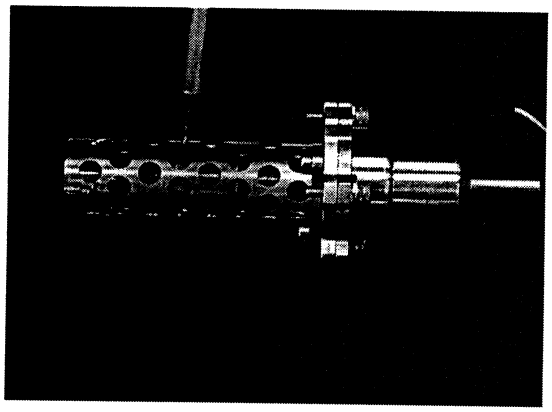

Figure 1: Moog Model 50X914 Resistojet

The resistojet consists of a solenoid valve for on/off propellant flow control, thermally insulated mounting interface, a heat exchanger, and expansion nozzle.

The valve is a no-sliding-fit, normally-closed solenoid operated valve based on Moog flight-qualified designs [2,3]. It is electrically energized open to initiate and maintain propellant flow to the heat exchanger and nozzle. The valve operates the resistojet in either continuous or pulsing modes. A filter is incorporated in the inlet port to protect the valve from contamination.

The goal of any resistojet design is to reduce the heat lost due to conduction and radiation. In the Moog model 50X914, conduction to the spacecraft and solenoid valve are reduced by using thin-wall members on either side of the resistive heater. On the downstream side of the heater, the nozzle wall is held intentionally thin to reduce heat loss in that direction. On the upstream side of the heater, a bellows minimizes conduction to the valve and spacecraft structure during pre-heat, operation, and after shutdown. The bellows purpose is actually three-fold. First, the bellows serves as a flow passage between the solenoid valve and the laminar flow element. Second, the thin-wall cross section of the bellows produces high thermal resistance. This reduces the conductive heat flow to the mounting interface. Third, the bellows is a compliant member able to change lengths in order to relieve stresses caused by differential thermal expansion.

The heat exchanger consists of both a resistive heat generator, and a unique laminar element, which efficiently transfers heat to the propellant. The heater uses a swaged nichrome heating element wrapped around a spool. The laminar flow element is pressed inside the spool. This allows for efficient heat transfer to the element and eliminates propellant from flowing between the spool and laminar element. The nominal heater resistance is 42 Ω and varies by only 2 % between room temperature and its full-power

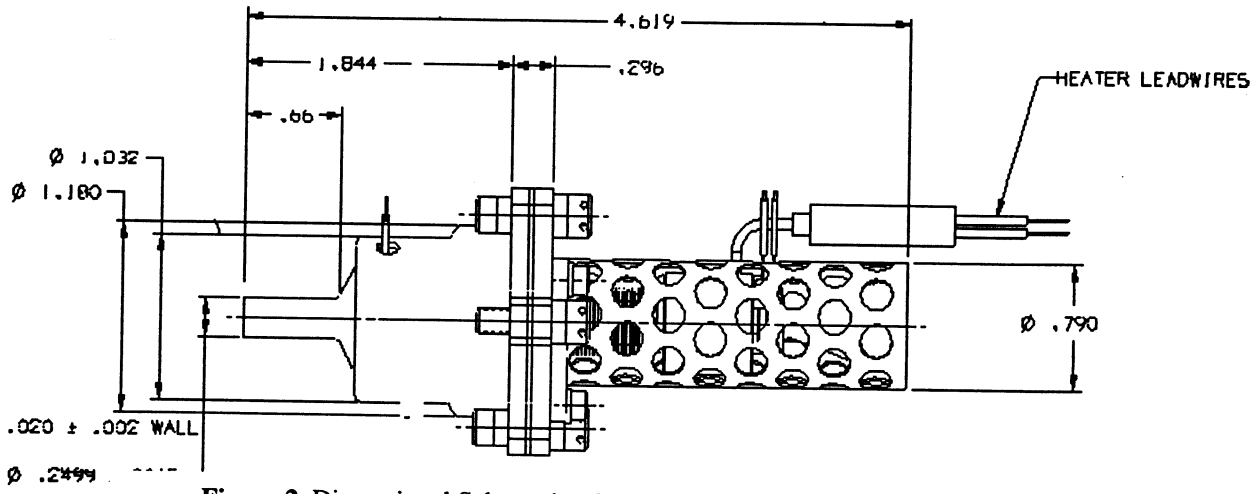

Figure 2 Dimensional Schematic of Moog Model 50X914 Resistojet

operating point.

The laminar flow element is of brazed copper design. The packed particle design forms a torturous path for the propellant working fluid. The gas passes through the element in multiple thin cross-sections for efficient heat transfer.

The completed heat exchanger section is pictured in Figure 3. The heat exchanger subassembly pictured is all welded to prevent external leakage. From left to right in the picture are: the resistojet mounting flange, thin-wall bellows, heater (with internal flow element), and expansion nozzle. The geometry chosen for the conical nozzle is a 17° half-angle design.

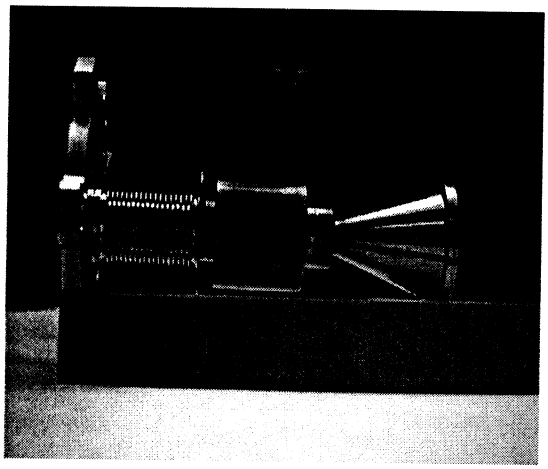

Figure 3: Heat Exchanger

Because the bellows has insufficient structural rigidity normal to its flow axis, a thin wall perforated tube surrounds the heat exchanger for structural support. Additionally, the perforated tube is designed to produce reliable nozzle position in relation to the mounting interface.

Heat Exchanger Analysis

The analysis of resistojet performance must consider both the pressure drops through the system and the final gas temperature prior to expansion through the nozzle. Figure 4 shows the pressure budget model.

Three separate pressure drops occur through the resistojet. The pressure drop through the valve (P1-P2) can be easily calculated by using subsonic orifice theory. The pressure drop through the expansion nozzle (P3-P4) can be calculated using supersonic orifice theory. These calculations are not presented in this paper.

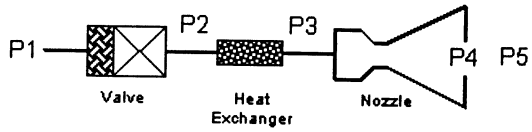

Figure 4: Resistojet Pressure Budget Model

The theoretical basis for calculating the pressure drop across the heat exchanger (P2-P3) comes from the Ergun equation shown as Equation 1[4]. The Ergun equation considers gas flow across packed spherical particles.

$$-\frac{dP}{dx} = 150\frac{(1-\varepsilon)^2}{\varepsilon^3}\frac{\mu G}{\rho D_P{}^2} + 1.75\frac{(1-\varepsilon)}{\varepsilon^3}\frac{G^2}{\rho D_P} \quad \text{.....(1)}$$

where
ε = Porosity

G = Mass Flux ($4*\dot{m}/\pi d^2$)
D_p = Particle diameter

This equation can be integrated to find ΔP across the length of the porous element. It is assumed that the porous element is subjected to uniform heating from the resistive heater. Therefore, the gas temperature at any axial location (x) is given by Equation 2.

$$T(x,L) = T_{IN} + (T_{OUT} - T_{IN})*\frac{x}{L} \qquad (2)$$

The gas is assumed to be ideal. Therefore, density can be expressed by the ideal gas law (Equation 3).

$$\rho(T) = \frac{P}{RT} \qquad (3)$$

Lastly, gas viscosity is assumed to vary in a predictable manner with temperature. A curve fit from published data[5] was used to quantify propellant viscosity as a function of temperature.

The curve fit for nitrogen and xenon took on the form of Equation 4. The constants are presented in Table 2.

$$\mu(T) = a + bT + cT^2 \qquad (4)$$

Table 2: Equation 4 Viscosity Constants for Test Gasses

	a ($x10^{-6}$)	b ($x10^{-8}$)	c ($x10^{-12}$)
Nitrogen	6.0	4.0	-9.0
Xenon	-0.5366	8.427	19.5

Equation 1 can be integrated subject to the constraints of Equations 2-4 to find pressure drop across the porous element. This equation is presented in Equation 5.

$$G = \frac{\frac{-150(1-\varepsilon)^2}{\varepsilon^3}\frac{R}{D_P^2}\int \mu(T)T(x)dx + \sqrt{\left(\frac{150(1-\varepsilon)^2}{\varepsilon^3}\frac{R}{D_P^2}\int \mu(T)T(x)dx\right)^2 - 3.5\frac{(1-\varepsilon)}{\varepsilon^3}\frac{R}{D_P}\left(P_{in}^2 - P_{out}^2\right)\int T(x)dx}}{3.5\frac{(1-\varepsilon)}{\varepsilon^3}\frac{R}{D_P}\left(P_{in}^2 - P_{out}^2\right)\int T(x)dx} \qquad (5)$$

In practice, a mass flow rate is assumed and the equation is iterated to determine the outlet pressure for a given inlet pressure. A similar equation was used in the design of the porous element to determine particle size D_p.

Heat Exchanger Experiments

The validity of the analysis presented in the preceding section was verified by experiment. A test fixture was fabricated which allowed temperature and pressure to be measured at the entrance and exit of the porous element. The test fixture used a dual heater design which could be disassembled so that the porous element could be changed. The experimental arrangement is shown in Figure 5.

The porous element was placed in the test fixture and subjected to a series of mass flow rates and input powers. A fine adjustment regulator was used to control inlet pressure to 24.7 psia. This pressure was chosen to match the anticipated inlet pressure in the resistojet application. The maximum applied power was 70 W.

A needle valve downstream of the test fixture controlled flow to the desired mass flow rate. Flow rate was measured with a Sierra mass flow meter calibrated for nitrogen. Inlet and outlet pressures were measured with separate Mensor pressure transducers and temperatures were measured with two type K thermocouples. All data were collected on a digital data acquisition system. Nitrogen was used as the test gas. The results of these tests are presented in Figure 6.

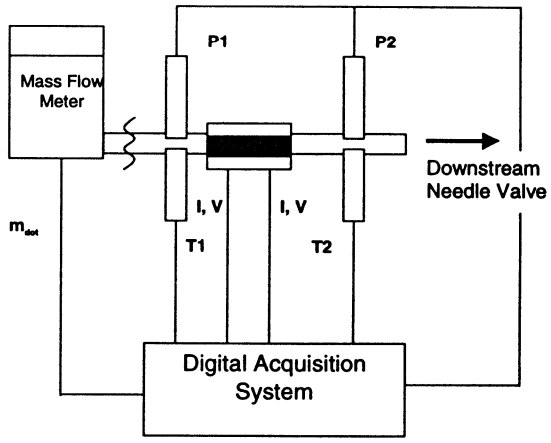

Figure 5: Heat Exchanger Experimental Arrangement

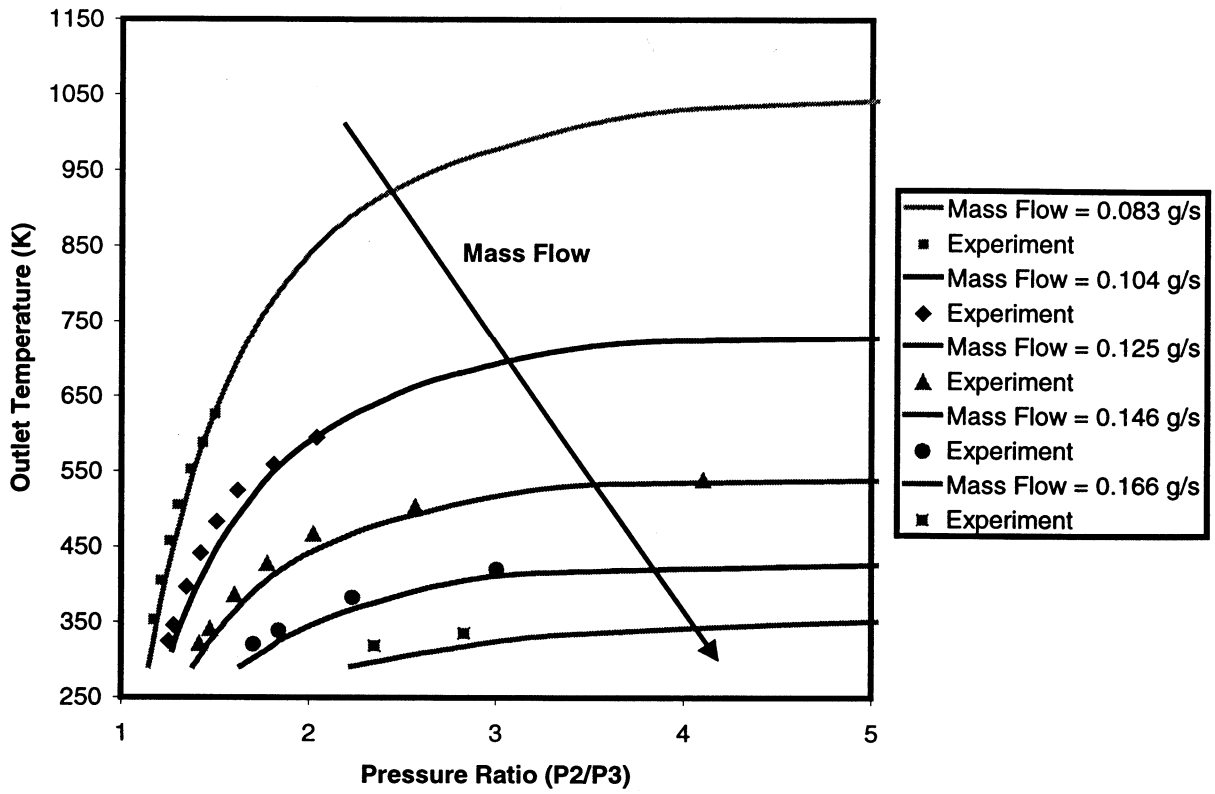

Figure 6: Temperature Versus Pressure Ratio of Nitrogen for Porous Element

In the Figure, the solid lines represent the analytical solution given by Equation 5 for the given mass flow rate. The data points are experimentally determined values. For each flow rate, the analysis predicts a maximum anticipated outlet temperature. The experimentally determined values track the asymptotic behavior predicted by the analysis.

The analysis needed to be corrected to account for increased inlet temperatures. As stated earlier, temperatures were taken on the inlet and outlet of the porous element. The inlet temperature measurements showed that the gas temperature was elevated prior to entering the porous element heat exchanger. This was obviously from heat gathered from the test fixture. The increased inlet temperature, which was not accounted for in designing the porous element, led to greater than anticipated viscous losses and lower outlet pressures. Failure to account for the increased inlet temperature in the analysis led to poor results when compared to the experiments.

Thrust and Specific Impulse Testing

Figure 7 shows a schematic of the experimental arrangement used for thrust and specific impulse testing.

Facility

The thrust and specific impulse tests were conducted in vacuum chamber 8 at NASA Glenn Research Center. A facility description can be found in the paper by Jankovsky[1]. Background pressure for all tests was held below 1 x 10^{-3} torr.

Thrust was measured on a precision flexure thrust stand. The deflection was recorded via the computer based data acquisition system and calibrated in-situ with previously measured weights.

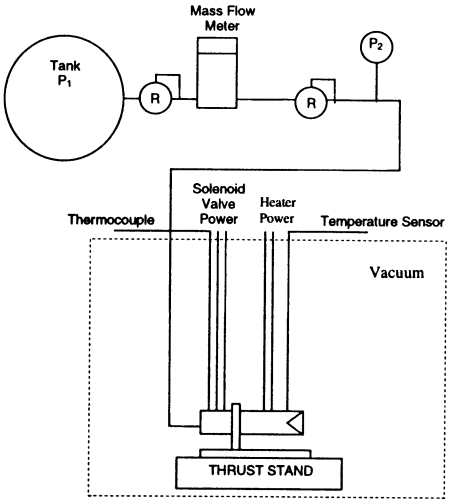

Figure 7: Experimental Arrangement for Thrust and Specific Impulse Testing

Experimental Apparatus

Moog used a similar test arrangement for the thruster testing as with the heated element testing. The regulator attached to the gas bottle regulated pressure to approximately 50 psia. Downstream of the bottle regulator, a needle valve was used to accurately control the pressure to the resistojet inlet. Between the two regulating devices was a Unit Instruments mass flow meter (0-10 SLM). The Unit Instruments meter was calibrated on nitrogen by the manufacturer and calibrated at the facility for xenon. It was positioned upstream of the needle valve so that it could remain at constant pressure. Inlet pressure was measured with a Mensor pressure transducer.

Two temperatures were measured during the testing. Heater temperature was monitored with a Rosemount resistance device (10 Ω ice point resistance) and solenoid valve body temperature was monitored with a type K thermocouple. Solenoid valve temperature were monitored to assure that there was no excessive heating from the heat exchanger.

Experimental Procedure

Data were collected for both nitrogen and xenon propellants. Initial tests were conducted without heater power at inlet pressures of 6, 12 18, 24, and 30 psia. For heated flow, the maximum power input to the heater was 70 W. For nitrogen, heater input powers of 10, 20, 30, 40, 50, 60, and 70 W were used. For xenon, heater input powers of 12.5, 25, 37.5, 50 and 70 W were used.

To start testing, the resistojet solenoid valve was commanded open and held open with approximately 1 W of power. The lowest power setting was applied to the resistojet heater at the lowest flow rate. No preheating of the heat exchanger was attempted. Data were recorded once the flow reached a steady condition. For most points the time required to reach steady operation was approximately 5 minutes. The inlet pressure was then increased to the next pressure setting. Once a sweep of pressures was completed, the power was increased to the next level. Figure 8 is a picture of the resistojet in operation on the NASA thrust stand.

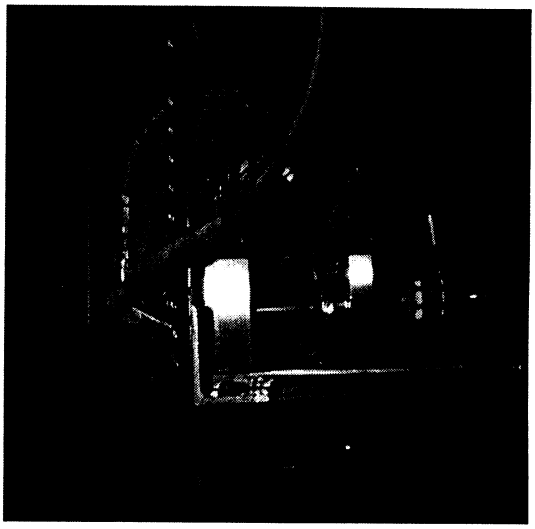

Figure 8: Moog Model 50X914 in Operation

Results

Thrust, input power, and mass flow rate were directly measured. Other performance values were calculated from these measured values. Specific Impulse was calculated in the customary way. Total Thruster Efficiency was defined as the ratio of the useful power output ($\frac{1}{2}\dot{m}v^2$) to the total (chemical and electrical) power input. Total Thruster efficency was calculated by 6.

$$\eta_T = \frac{gFI_{sp}}{2(P_{Input} + \dot{m}h)} \qquad (6)$$

Nitrogen
Testing on nitrogen was performed over a mass flow range of 0.0085 to .1804 g/s. The maximum measured thrust was 152 mN and highest specific impulse was 115.2 s at 70 W of heater power. Figures 9 and 10 show the experimental results of the resistojet performance with nitrogen.

Figure 9 shows the resistojet specific impulse as a function of thrust. At the higher thrust levels, there are nearly vertical lines of data which correspond to inlet pressure. The higher specific impulses at similar thrusts are measured for higher heater powers. In each case, maximum specific impulse was observed at the more moderate pressures (12 to 24 psia). At lower thrusts nozzle effects appear to degrade resistojet performance. This is particularly true for the higher power test conditions.

Figure 10 shows thruster efficiency as a function of thrust. At each power level, the thruster efficiency increases at higher thrusts. The total thruster efficiency at each power level appears to be asymptotically approaching approximately 75%. At each flow rate, thruster efficiency is higher for the lower power input.

Xenon
Testing on xenon was performed over a mass flow range of 0.023 to .484 g/s. The maximum measured thrust was 132.5 mN and highest specific impulse was 66.9 s at 70 W of heater power. Figures 11 and 12 show the experimental results of the resistojet performance with xenon.

Figure 11 shows the resistojet specific impulse as a function of thrust. Like Figure 9 for nitrogen, there are nearly vertical lines of data which correspond to inlet pressure. The higher specific impulses at similar thrusts are measured for higher heater powers.

Figure 12 shows thruster efficiency as a function of thrust. At each power level, the thruster efficiency increases at higher thrusts where nozzle effects are reduced.

Conclusions

Moog, Inc. performed development testing on a resistojet with both nitrogen and xenon propellants. At 70 W heater power and 30 psia inlet pressure the thrust was measured to be 127 mN at a mass flow rate of 0.277 g/s. The mass flow rate through the porous element fell short of the design condition. Preheating of the gas prior to arriving at the porous element increased gas viscosity resulting in greater viscous losses through the porous element. The lower than anticipated mass flow rate resulted in insufficient pressure upstream of the sonic orifice (P3) and thus low thrust. Specific impulses on xenon were measured to be as high as 66.9 s at 70 W.

Acknowledgments

Moog gratefully acknowledges NASA Glenn Research Center for funding this work under contract number NAS3-98130 and their aid in the development testing.

References

1. Jankovsky, R., Sankovic, J., and Oleson, S., "Performance of a FAKEL K10K Resistojet," AIAA 97-3059, 33rd AIAA/ASME/SAE/ASEE Joint Propulsion Conference, Seattle, WA, July, 1997.

2. Bushway, E.D. and Rogers, W.P., "Minature Lightweight Propellant Management Assembly for Stationary Plasma Thrusters," AIAA 97-2788, 33rd Joint Propulsion Conference, Seattle, WA, 1997.

3. Bushway, E.D., Engelbrecht, C.S., and Ganapathi, G.B., " NSTAR Ion Engine Xenon Feed System: Introduction to System Design and Development," IEPC-97-044, 25th International Electric Propulsion Conference, Cleveland, OH, 1997.

4. Bird, R.B., Stewart, W.E., and Lightfoot, E.N., Transport Phenomena, John Wiley and Sons, New York, (1960), p. 200.

5. Vargaftik, N.B., Tables on the Thermophysical Properties of Liquids and Gases, John Wiley and Sons, New York, (1975).

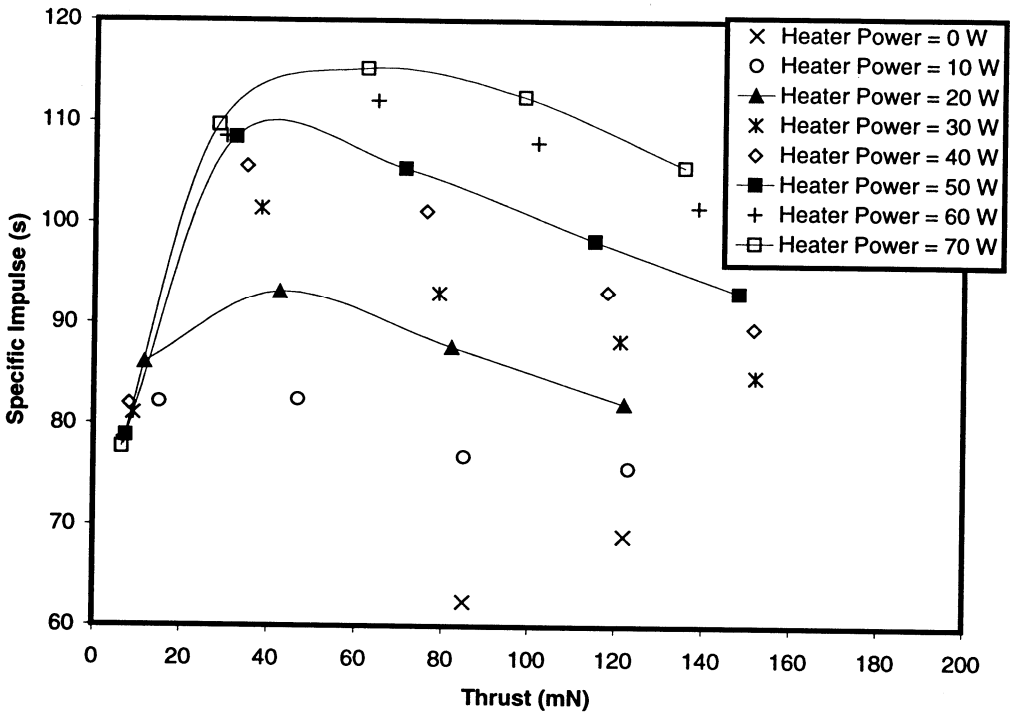

Figure 9: Specific Impulse versus Thrust for Moog Model 50X914 Operating on Nitrogen

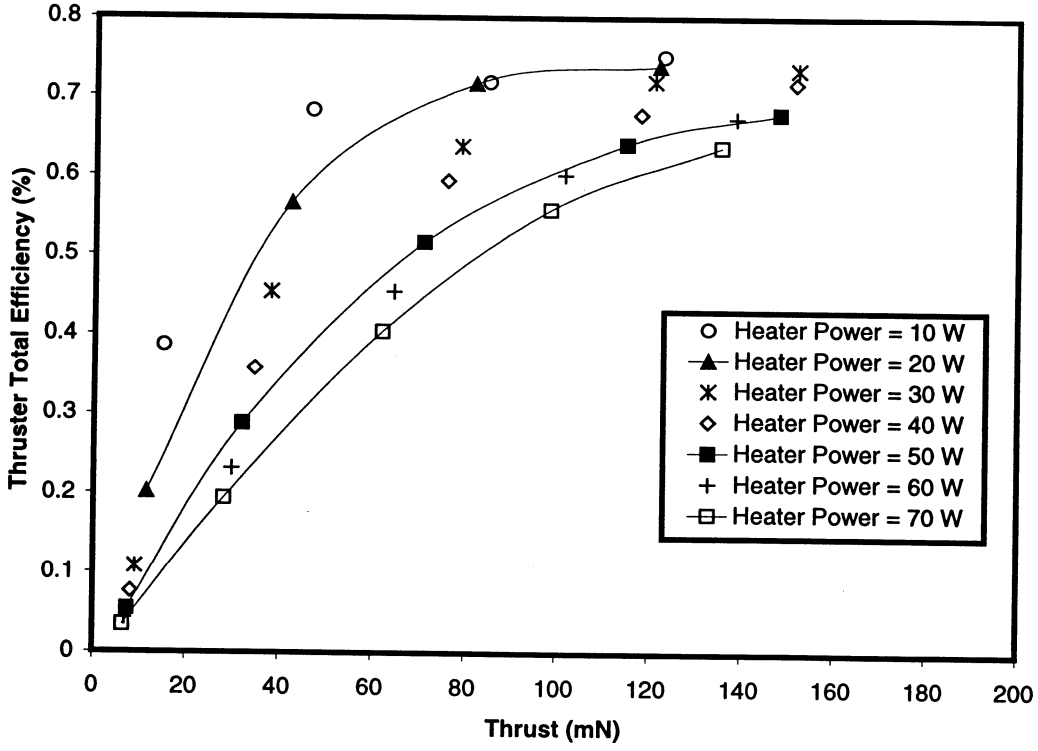

Figure 10: Thruster Total Efficiency versus Thrust for Moog Model 50X914 Operating on Nitrogen

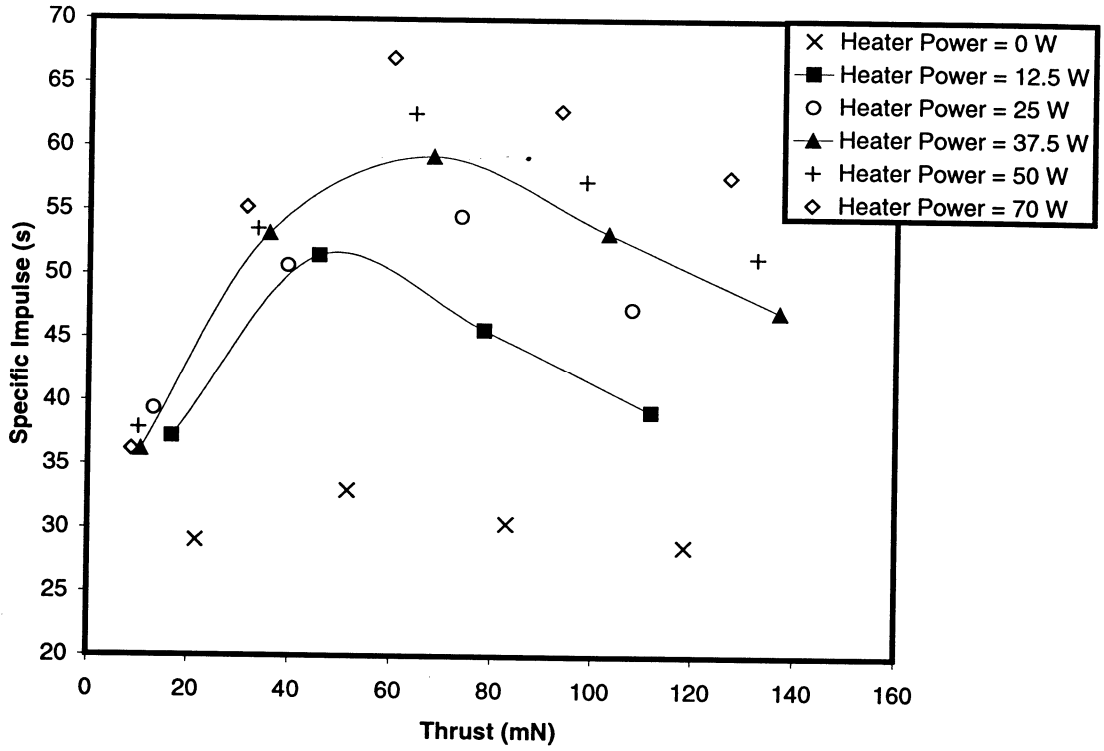

Figure 11: Specific Impulse versus Thrust for Moog Model 50X914 Operating on Xenon

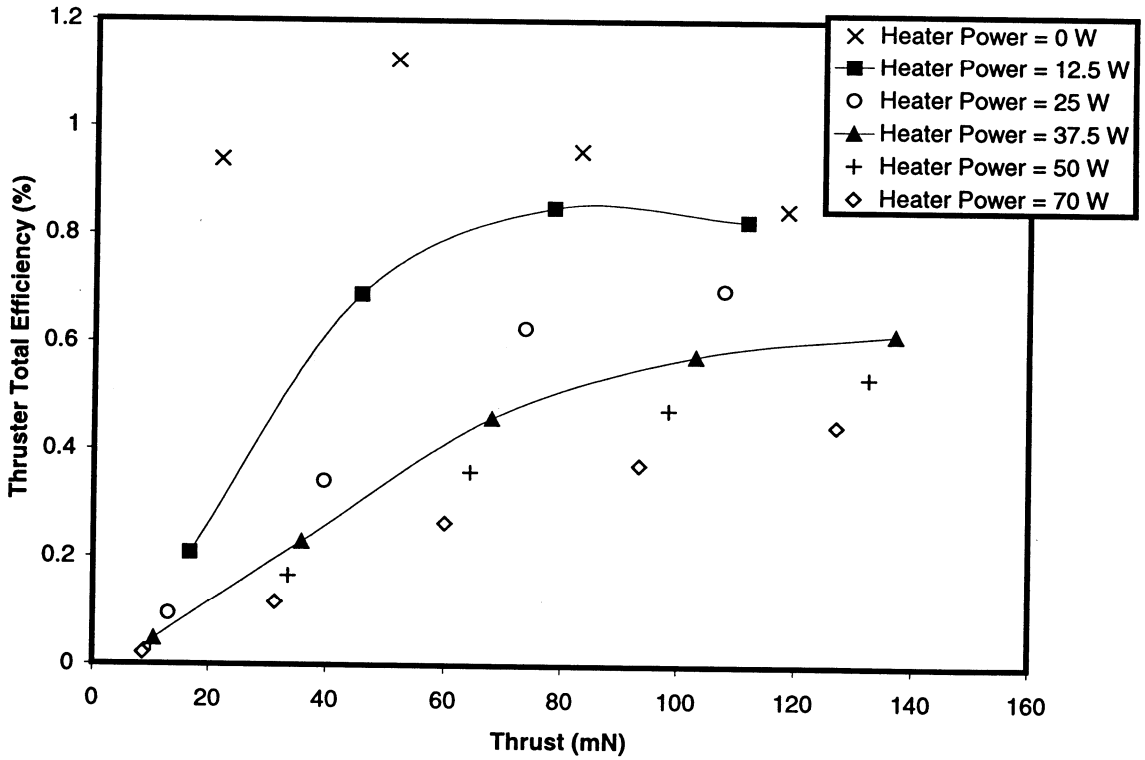

Figure 12: Thruster Total Efficiency versus Thrust for Moog Model 50X914 Operating on Xenon